Eur Biophys J (2004) 33: 726–731
DOI 10.1007/s00249-004-0418-z

ARTICLE

**Elena Casero · José A. Martín-Gago · Félix Pariente
Encarnación Lorenzo**

Metal release in metallothioneins induced by nitric oxide: X-ray absorption spectroscopy study

Received: 2 March 2004 / Revised: 23 April 2004 / Accepted: 3 May 2004 / Published online: 4 June 2004

Abstract Metallothioneins (MTs) are low molecular weight proteins that include metal ions in thiolate clusters. The capability of metallothioneins to bind different metals has suggested their use as biosensors for different elements. We study here the interaction of nitric oxide with rat liver MTs by using in situ X-ray absorption spectroscopy techniques. We univocally show that the presence of NO induces the release of Zn atoms from the MT structure to the solution. Zn ions transform in the presence of NO from a tetrahedral four-fold coordinated environment in the MT into a regular octahedral six-fold coordinated state, with interatomic distances compatible with those of Zn solvated in water.

Keywords EXAFS · Metallothionein · Nitric oxide · XANES · Zinc

Introduction

Metallothioneins (MTs) are ubiquitous and very unusual proteins present in a broad range of species, which have focused the interest of chemists and biochemists over the last three decades. This interest is due to the special characteristics of this family of polypeptides, summarized by the following chemical properties: (1) low molecular weight (6000–7000 Da); (2) high metal content; (3) great number of cysteine residues in the primary structure; and (4) arrangement of metal ions in oligonuclear metal thiolate complexes (clusters) (Suzuki et al. 1993). Based on their structural design, MTs show great stability at high temperatures and in moderately high acidic or alkaline solutions (Hamer 1986). The mammalian MTs consist of a single polypeptide chain of 61 or 62 amino acid residues, of which 20 are cysteines located in highly conserved positions. All the cysteine residues are coordinated to metal ions via metal–thiolate bonds, giving rise to spectroscopic properties characteristic of metal thiolate clusters; each protein molecule has capability to bind 7 equivalents of divalent metal ions. The protein is formed by two clusters, one with four divalent ions and other with three ions, all of them bound by four thiolate ligands arranged in tetrahedral symmetry.

Many physiological roles have been proposed for these proteins, including detoxification of heavy metals, homeostasis of essential trace metals and scavenging of free radicals (Sato and Bremner 1993). Since one of the most important features of MTs is their capacity to bind essential metals like copper and zinc, as well as cytotoxic heavy metals such as cadmium, mercury and silver, they are considered as potential biomarkers of environmental metal contamination (Roesijadi 1996). It is worth to consider also the potential roles of MTs as redox sensors based on their high sensitivity to cysteine modification, as well as their potential to amplify signals by releasing multiple metal ions (Fabisiak et al. 2002). The great versatility of MTs to bind metals or free radicals such as nitric oxide (St Croix et al. 2002 and references therein) makes them very useful in the development of biosensors since MTs can be used as the biorecognition layer in such devices.

In the last few years there has been an increasing interest in the development of methods for detecting and monitoring nitric oxide (NO), because of its importance in clinical and environmental analysis. The ability to travel rapidly between cells and its short half-life makes NO ideal in intercell communication such as in the central and peripheral nervous system and in host defense mechanisms of eukaryotes (Marletta et al. 1990; Edelman and Gally 1992; Moncada 1992). Among other important functions, NO can act as a neurotransmitter

J. A. Martín-Gago (✉)
Instituto Ciencia de Materiales de Madrid, CSIC,
28049 Cantoblanco, Madrid, Spain
E-mail: gago@icmm.csic.es
Fax: +34-91-3720623

E. Casero · F. Pariente · E. Lorenzo
Departamento de Química Analítica y Análisis Instrumental,
Universidad Autónoma de Madrid, 28049 Cantoblanco,
Madrid, Spain

(O'Dell et al. 1991), prevent platelet aggregation (Radomski et al. 1990) and play an important role in the immune system against tumor cells (Hibbs et al. 1988) and intracellular bacteria (Hibbs et al. 1987).

Despite the great interest in the determination of NO production, most of the methods used for its determination are indirect, relying on measurements of secondary species, such as breakdown products of NO metabolism (nitrite and nitrate). Bioassays based on the physiological effects of NO have been also proposed. In this way, biosensors are highly selective devices, which rely on the specific binding of the target analyte to the biorecognition layer. In the case of MTs, it is clear that in order to develop technological applications such as biosensors for NO determination, based on the high affinity of MTs to NO, knowledge and control of the protein/NO interaction is essential. In this way, in the present work, we have investigated at the atomic level the nature of Zn binding sites on MTs in the presence and absence of NO using in situ X-ray absorption near edge spectroscopy (XANES) and extended-X-ray absorption fine structure (EXAFS). X-ray absorption spectroscopy (XAS) has been extensively employed to probe the structure of metalloproteins (Jiang et al. 1994), as well as to follow in situ structural changes in low concentrated solutions of proteins. These are very suitable techniques to obtain information about local structural transformations taking place around metallic atoms, and therefore they are appropriate to study the interaction between MTs and radicals or metals. XANES gives information on the identity of the metal and its valence whilst EXAFS gives quantitative information on the ligand environment. The aim of the present work is to use the power of these techniques to study the interaction of NO with rat liver MTs in solution, as a preliminary work in the design of biosensors for NO determination. In this sense, we will show that the presence of NO induces the release of Zn atoms of MTs into solution.

Materials and methods

Reagents

Metallothionein 2 (MT2) used in the present work was purified from liver of Sprague Dawley rats that were previously administered subcutaneously with $CdCl_2$ (3.0 mg of Cd per kg of body weight) over a period of 14 days. The purification procedure and further characterization of the MT2 fractions has been described in detail elsewhere (Casero et al. 2002). The metal content of these protein samples was estimated from atomic absorption measurements. According to the results, a stoichiometry of Zn_2Cd_5-MT2 was found. High-purity NO was purchased from Air Liquide. Standard saturated NO solutions were prepared by bubbling NO gas through oxygen-free buffer solution for 30 min. Aliquots of this saturated solution were used to prepare solutions of known NO concentration, using a value of 1.9 mM for its concentration at saturation (Gerrard 1980). Other chemicals used in the present work were reagent grade quality. Water was purified with a Millipore Milli-Q system. All solutions were prepared just prior to use.

Sample preparation

For XAS measurements, 0.3 mM $Zn(NO_3)_2$ aqueous solutions were used as reference samples (from now on, will be referred in the figures as Zn). The Zn spectrum in MT2 was measured in a 0.15 mM MT2 solution freshly prepared by diluting a stock solution of MT2 (4.0 mM) with water. To study the effect of nitric oxide on MT2, aliquots of 4.0 mM MT2 stock solution and 1.9 mM NO solution were mixed in the absence of oxygen to give rise to a final solution containing 0.15 mM MT2 and 1.3 mM NO in water. This solution was prepared immediately before use. It is important to note that the concentration of Zn ions in the three types of samples was 300 μM.

Instrumentation and XAS measurements

The zinc and cadmium content of purified MT2 samples was determined by atomic absorption spectroscopy using a Varian Spectr AA-640Z spectrometer. In XAS experiments the MT solution was contained in a cell closed by a Kapton window with a total sample capacity around 100 μL.

The Zn K-edge absorption measurements were performed at the European Synchrotron Radiation Facility (ESRF), on beamline ID26, equipped with an undulator source and energy dispersive optics. Data were collected in transmission mode, recording beam intensities I_0 and I before and after the sample by using photodiodes. A Si(111) crystal was used as monochromator, yielding an intrinsic resolution ($\Delta E/E$) of $\sim 10^{-4}$ and a horizontal spot size of ~200 μm. The sample was at room temperature during the experiments. Special care was paid to check for the absence of damage induced by the X-ray radiation. Particularly, a beam shutter was set up to reduce the sample exposure time during data acquisition. Also, fast control scans were recorded, intercalated to ensure the nonexistence of lineshape changes induced by beam damage.

Data processing

The absorption spectra were obtained by averaging 20 different measurements recorded from 9500 to 10500 eV. EXAFS spectra were treated following a standard procedure (Teo 1986) by means of a chain of programs written by Michalowicz (1990, 1991) and Noinville and Michalowicz (1991). The EXAFS contribution was calculated by taking E_0 equal to the energy at half the edge jump (9661.9 eV in the MT sample and 9664.9 eV in the MT + NO sample) and was obtained using the following expression:

$$\chi(E) = (\mu(E) - \mu_1(E))/((\mu_1)(E) - \mu_0(E)) \tag{1}$$

where $\mu(E)$ is the observed absorption, $\mu_0(E)$ is the background absorption calculated by using a theoretical expression developed by Lengeler and Eisenberg (1980) and $\mu_1(E)$ is the atomic absorption approximated by a fifth polynomial expression. The pseudo-radial distribution functions (RDF) were found after the application of a Kaiser window ($\tau = 2.5$; $k = 2.4$–13.2 Å^{-1} in the MT sample and $k = 1.8$–14.1 Å^{-1} in the MT + NO sample) to the $k^2\chi(k)$ data Fourier transform.

Results and discussion

The MT2 purification procedure involves zinc and cadmium ions as the metals associated with the protein preparations (Casero et al. 2002). The metal content of these preparations was determined by atomic absorption spectroscopy. According to our results, a stoichiometry of 5 mol of Cd and 2 mol of Zn per mol of protein was observed. This stoichiometry has been reported by other authors in rat liver MTs purified following similar procedures (Furey et al. 1986). In addition, the structure of Cd_5Zn_2-MT2 from rat liver has been studied by X-ray diffraction in single crystals (Furey et al. 1987; Robbins et al. 1991) and by NMR spectroscopy in solution (Schultze et al. 1988; Messerle et al. 1990). According to these studies (Braun et al. 1992), MT2 contains exclusively four Cd^{2+} ions in the α-domain, the β-domain contains two Zn^{2+} ions and one Cd^{2+} ion, and in the single crystals there is also observed the presence of one Na^+ ion in the β-domain (Fig. 1).

As mentioned above, MTs are involved in some protective mechanisms in living cells, in addition to such unspecified protective functions against toxic heavy metals (like cadmium). Recent findings imply that liver MT2 may have a more specific role in Zn-related cellular processes in response to signals for cell activation or in the presence of chemical messengers, such as NO. This inorganic molecule is able to form nitroso thiols with cysteine residues in MT2 and in consequence probably is capable of releasing the Zn^{2+} ions from the native MT2.

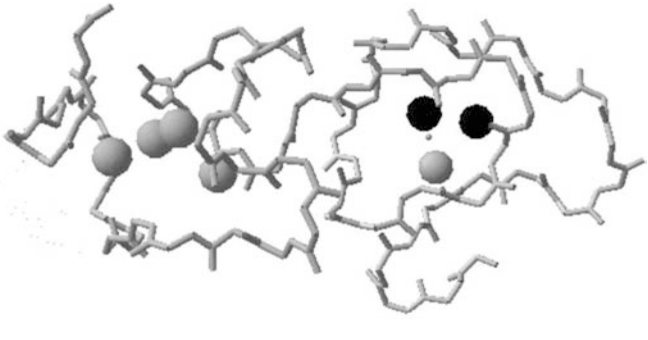

Fig. 1 Structure of rat liver Zn_2Cd_5-MT2 according to Braun et al. (1992). *Black balls* represent Zn atoms and *gray balls* Cd

On the other hand, XANES and EXAFS have been previously used to probe the atomic Zn geometrical structure in different liquid environments (Ludwing et al. 1987; Jones et al. 1994; D'Angelo et al. 2002a, 2002b; Simonet et al. 2002). These techniques allow us to gather precise information about the nature, number and distance of the different atoms located near a selected atom, in our case, Zn. The coordination chemistry of Zn is quite simple. Zn is most often four- or six-fold coordinated. Its d^{10} electronic configuration implies isotropic chemical bonds and regular polyhedra. Consequently, in a given structural environment, metal–ligand interatomic distances are homogeneous. Distances for Zn–O pairs in tetrahedral coordination are different than in octahedral coordination. The Zn–O distances range from 1.90 to 2.00 Å for the four-fold coordination and from 2.00 to 2.20 Å for the six-fold coordination (Sarret et al. 1998). Distances for Zn–S pairs (which is the case for MTs) are 0.2–0.3 Å longer than Zn–O pair distances (corresponding to Zn in solution), as a result of the difference in ionic radius between O (1.26 Å) and S (1.84 Å) (Shannon and Prewitt 1969; Shannon 1976). Thus, O and S neighbors can be differentiated on the basis of interatomic distances. In addition, it is well known that neighboring atoms can be also identified through their different backscattering properties, which depend on their atomic number. In our case, S has twice the number of electrons as O; this is different enough to allow us to discriminate between them.

XANES study

Figure 2 shows the Zn K absorption edge spectra of three different Zn solutions. These spectra are normalized to the incident flux and total jump. The upper spectrum corresponds to a 0.3 mM $Zn(NO_3)_2$ solution in water. A sharp peak close to the absorption edge characterizes this spectrum. The shape of the peak is similar to that reported by D'Angelo et al. (2002b). These authors have fitted, by multiple scattering calculations, the fine structure of the spectrum, leading to a precise determination of the well-known regular octahedral configuration of the water molecules around the ions. From this analysis they found a Zn–O distance of 2.06 ± 0.03 Å. The spectrum at the bottom shows the Zn K edge from a 0.15 mM MT2 solution. This spectrum presents a completely different shape, indicating a different structural arrangement of the Zn atoms. In fact, Zn atoms in MT are coordinated in a tetrahedral arrangement with sulfur atoms. The spectrum in the middle of the figure was obtained after dosing a previous MT2 stock solution with NO, as described in the Materials and methods section. The line shape is remarkably close to that of Zn in solution (upper curve, Fig. 2), indicating a similar environment for the Zn atoms. The conclusion that can be drawn from this

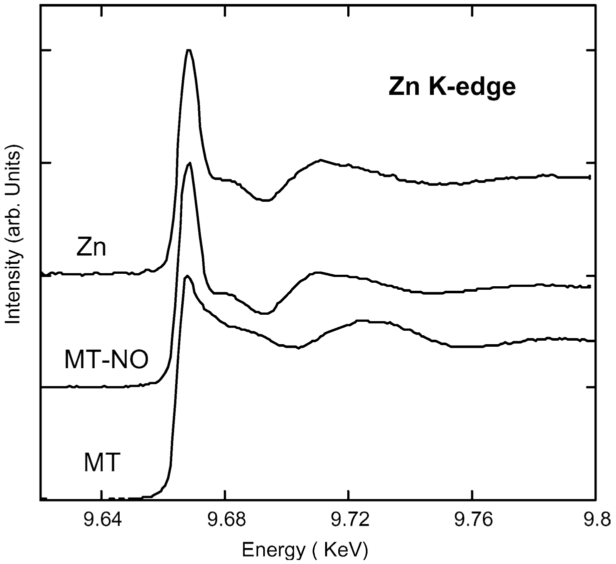

Fig. 2 Zn K-edge absorption spectra (XANES) of three different Zn solutions. *Upper spectrum*: Zn nitrate solution; *lower*: MT solution; *middle*: NO added to a MT solution

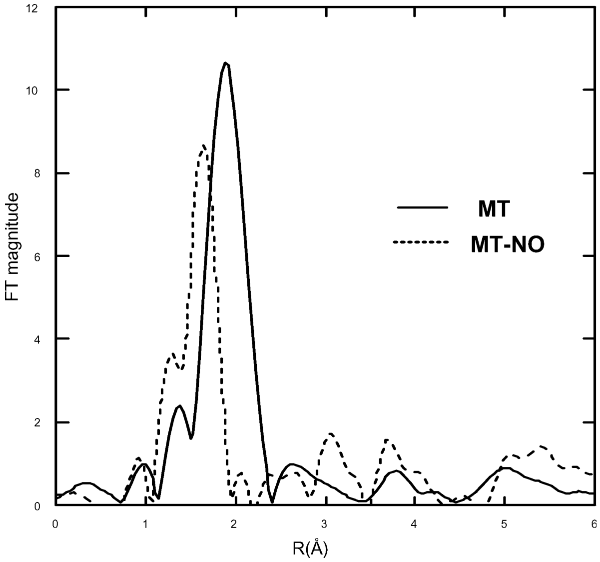

Fig. 3 Pseudo-radial distribution function of Zn K-edge calculated by Fourier transform of EXAFS spectra from MT (*solid line*) and MT + NO (*dashed line*)

observation is straightforward: the presence of NO in the solution induces the release of Zn atoms from the S cluster into the solution, where they arrange into an octahedral coordination with OH molecules.

Furthermore, since the Zn concentration in the spectra of Fig. 2 is the same and we do not observe any spectroscopic signature in the central spectrum corresponding to MT, we conclude that the presence of NO mostly removes the Zn from the MT to the solution. Finally, we would like to remark that a similar result was obtained for MT1, indicating that the environment of the Zn–S groups in both MT isoforms is very similar.

EXAFS study

The qualitative results indicated by NEXAFS have been confirmed and quantified by an EXAFS study. The EXAFS signal provides precise information about identity, distance and number of atoms that surround an absorbing element. Figure 3 shows the pseudo-radial distribution function (RDF) of a MT solution before and after addition of an aliquot of NO.

Both curves contain a single intense peak for distances smaller than 6 Å, indicating a unique structural environment. For the spectrum corresponding to the MT, this peak appears at the shift-uncorrected distance of 1.90 Å. This distance is reduced to 1.67 Å after adding NO to the solution. The shortening of the bond distance is in good agreement with the previous scenario suggested by XANES. In fact, the released Zn coordinates to OH molecules, resulting consequently in a reduction of the first near-neighbor distance.

The main peaks of the two samples are accompanied by a shoulder at 1.40 Å and 1.31 Å for MT and MT-NO, respectively. These values are too short to correspond to physical bond lengths and hence we do not consider these peaks as real structural features but as residual background. We would like to emphasize that the data have been acquired on Zn concentrations of about 150 μM, and therefore the residual background is high. The absence of any other significant peak that could be interpreted as a second shell indicates that in both cases the system does not present long-range order (Jiang et al. 1994).

We have extracted the Fourier filtered contributions of the first coordination shell through an inverse transform from 1.12 to 2.33 Å in the MT sample and from

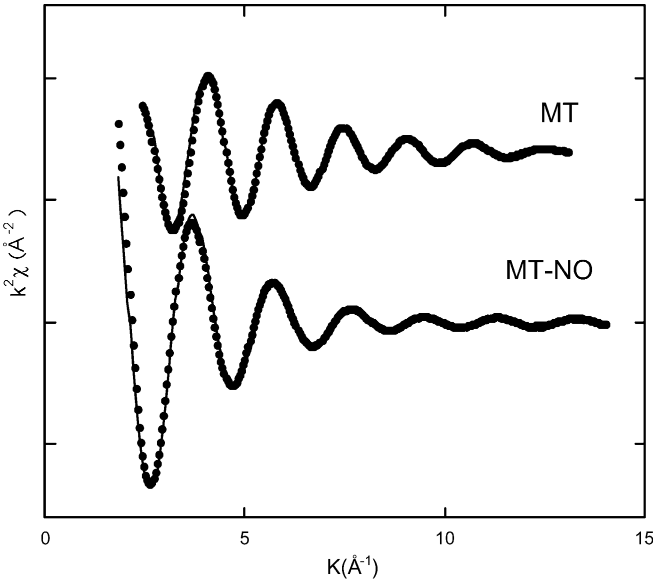

Fig. 4 Normalized Zn K-edge EXAFS of MT and MT + NO. *Solid lines* show the k^2–raw EXAFS data and *dotted lines* the result of the best fit with the relevant parameters summarized in Table 1

Table 1 Structural values [N = coordination number; R = mean distance of the neighbors (oxygen or sulfur) around the Zn; σ = Debye–Waller factor] obtained by fitting the experimental EXAFS data of Fig. 4 with other values from Jiang et al. (1994) and D'Angelo et al. (2002b)

	MT sample (this work)	MT + NO sample (this work)	MT (from Jiang et al. 1994)	Zn^{2+} in water solution (from D'Angelo et al. 2002b)
N	4.0 ± 0.3	6.1 ± 0.2	4.2 ± 0.5	6.0 ± 0.1
R (Å)	2.33 ± 0.02	2.08 ± 0.02	2.35 ± 0.01	2.078 ± 0.002
$\sigma(\text{Å}^2)\times10^{-3}$	6.6 ± 1	8.1 ± 1	4.2 ± 0.8	8.7 ± 0.5

1.03 to 1.91 Å in the MT + NO sample. We have determined, by fitting the k^2 weighted EXAFS spectra of the MT and the MT-NO samples (Fig. 4), the mean distance (R) of the neighbors (oxygen or sulfur) around the Zn, the coordination number (N) and the Debye–Waller factor (σ).

The relevant structural parameters (N, R and σ) and their corresponding errors obtained from the best-fit results are presented in Table 1. The values derived from this work are shown together with some structural results obtained in previous studies and they are in close agreement. The experimental and calculated spectra can be seen in Fig. 4. The experimental data from previous studies for both Zn in metallothionein (Jiang et al. 1994) and Zn in water (D'Angelo et al. 2002b) show similar absorption features to that presented in the upper and lower curves of Fig. 4, respectively.

The nearest neighbor distance for Zn–S in Zn-MT is estimated to be 2.33 Å, and the thiolate coordination 4, in accord with the thiolate environment of the Zn in the MT. These values are in close agreement with previously reported EXAFS work (2.35 Å) (Jiang et al. 1994). Addition of NO to the MT solution changes the coordination number to 6 and induces a reduction of the interatomic distance to 2.08 Å, which is in accord with the octahedral environment of the Zn atoms in aqueous solution, where a distance of 2.078 Å has been reported by a recent EXAFS study (D'Angelo et al. 2002b).

The release of the Zn atoms from the MT mediated by the presence of NO can undergo two possible mechanisms, according to the results published by other authors. Aravindakumar et al. (1999) describe that NO mediates Zn release from MT by destroying zinc-sulfur clusters, in contrast to the common belief that Zn release in presence of NO is due to the formation of a *S*-nitrosylate MT (Kroencke et al. 1994). In our case the technical limitation of the beamline used in these experiments did not allow us to draw any further conclusions about the N environment in the MT, and therefore to confirm any mechanism.

Conclusions

We have shown the ability of XAS techniques to obtain powerful in situ information about structural changes taking place in MTs, which could be employed for biosensor design. In this sense, we proved that the dosing of NO in a liquid containing MT induces the complete release of the Zn atoms from the MT shell to the solution.

Acknowledgements We acknowledge Thomas Neissius for technical assistance during measurements. This work has been funded by the Spanish research project MAT2002-395.

References

Aravindakumar CT, Ceulemans J, De Ley M (1999) Nitric oxide induces Zn^{2+} release from metallothionein by destroying zinc-sulphur clusters without concomitant formation of S-nitrosothiol. Biochem J 344:253–258

Braun W, Vasak M, Robbins AH, Stout CD, Wagner G, Kagi JH, Wuthrich K (1992) Comparison of the NMR solution structure and the X-ray crystal structure of rat metallothionein-2. Proc Natl Acad Sci USA 89:10124–10128

Casero E, Vázquez L, Martín-Benito J, Morcillo MA, Lorenzo E, Pariente F (2002) Immobilization of metallothionein on gold/mica surfaces: relationship between surface morphology and protein-substrate interaction. Langmuir 18:5909–5920

D'Angelo P, Barone V, Chillemi G, Sanna N, Meyer-Klaucke W, Pavel NV (2002a) Hydrogen and higher shell contributions in Zn^{2+}, Ni^{2+}, and Co^{2+} aqueous solutions: an X-ray absorption fine structure and molecular dynamics study. J Am Chem Soc 124:1958–1967

D'Angelo P, Benfatto M, Della Longa S, Navel NV (2002b) Combined XANES and EXAFS analysis of Co^{2+}, Ni^{2+}, and Zn^{2+} aqueous solutions. Phys Rev B 66:64209/1–64209/7

Edelman GM, Gally JA (1992) Nitric oxide: linking space and time in the brain. Proc Natl Acad Sci USA 89:11651–11652

Fabisiak JP, Borisenko GG, Liu Shang-Xi, Tyurin VA, Pitt BR, Kagan VE (2002) Redox sensor function of metallothioneins. Methods Enzymol 353:268–281

Furey WF, Robbins AH, Clancy LL, Winge DR, Wang BC, Stout CD (1986) Crystal structure of Cd,Zn metallothionein. Science 231:704–710

Furey WF, Robbins AH, Clancy LL, Winge DR, Wang BC, Stout CD (1987) Crystal structure of cadmium-zinc metallothionein. Experientia Suppl 52:139–148

Gerrard W (1980) Gas solubilities: widespread applications. Pergamon, Oxford

Hamer DH (1986) Metallothionein. Annu Rev Biochem 55: 913–951

Hibbs JB Jr, Vavrin Z, Tainton RR (1987) L-Arginine is required for expression of the activated macrophage effector mechanism causing selective metabolic inhibition in target cells. J Immunol 138: 550–565

Hibbs JB Jr, Tainton RR, Vavrin Z, Mrachlin EM (1988) Nitric oxide: a cytotoxic activated macrophage effector molecule. Biochem Biophys Res Commun 157:87–94

Jiang DT, Heald SM, Sham TK, Stillman MJ (1994) Structures of the cadmium, mercury, and zinc thiolate clusters in metallothionein: XAFS study of Zn_7-MT, Cd_7-MT, Hg_7-MT, and Hg_{18}-MT formed from rabbit liver metallothionein 2. J Am Chem Soc 116:11004–11013

Jones WB, Elgren TE, Morelock MM, Elder RC, Wilcox DE (1994) Technetium metallothionein: spectroscopic and EXAFS study of $^{99}TcO^{3+}$ binding to Zn_7-metallothionein. Inorg Chem 33:5571–5578

Kroencke KD, Fehsel K, Schmidt T, Zenke FT, Dasting I, Wesener JR, Betermann H, Breunis KD, Kolb-Bachofen V (1994) Nitric oxide destroys zinc-sulfur clusters inducing zinc release from metallothionein and inhibition of the zinc finger-type yeast transcription activator LAC9. Biochem Biophys Res Commun 200:1105–1110

Lengeler B, Eisenberg P (1980) Extended X-ray absorption fine structure analysis of interatomic distances, coordination numbers, and mean relative displacements in disordered alloys. Phys Rev B 21:4507–4520

Ludwing KF Jr, Warburton WK, Fontaine A (1987) X-ray studies of concentrated aqueous solutions. J Chem Phys 87:620–629

Marletta MA, Tayeh MA, Hevel JM (1990) Unraveling the biological significance of nitric oxide. Biofactors 2:219–225

Messerle BA, Schaffer A, Vasak M, Kagi JH, Wuthrich K (1990) Three-dimensional structure of human $[^{113}Cd_7]$metallothionein-2 in solution determined by nuclear magnetic resonance spectroscopy. J Mol Biol 214:765–779

Michalowicz A (1990) Thesis, Université de Paris Val de Marne

Michalowicz A (1991) Logiciels pour la Chimie. Societé Française de Chimie, Paris, p 102

Moncada S (1992) The 1991 Ulf von Euler lecture. The L-arginine:nitric oxide pathway. Acta Physiol Scand 145: 201–227

Noinville V, Michalowicz A (1991) Logiciels pour la Chimie. Société Française de Chimie, Paris, p 148

O'Dell TJ, Hawkins RD, Kandel ER, Arancio O (1991) Tests of the roles of two diffusible substances in long-term potentiation: evidence for nitric oxide as a possible early retrograde messenger. Proc Natl Acad Sci USA 88:11285–11289

Radomski MWJ, Palmer RM, Moncada S (1990) An L-arginine/nitric oxide pathway present in human platelets regulates aggregation. Proc Natl Acad Sci USA 87:5193–5197

Robbins AH, McRee DE, Williamson M, Collett SA, Xuong NH, Furey WF, Wang BC, Stout CD (1991) Refined crystal structure of cadmium-zinc metallothionein at ANG resolution. J Mol Biol 221:1269–1293

Roesijadi G (1996) Metallothionein and its role in toxic metal regulation. Comp Biochem Physiol C 113:117–123

Sarret G, Manceau A, Spadini L, Roux J, Hazemann J, Soldo Y, Eybert-Bérard L, Menthonnex JJ (1998) Structural determination of Zn and Pb binding sites in *Penicillium chrysogenum* cell walls by EXAFS spectroscopy. Environ Sci Technol 32:1648–1655

Sato M, Bremner I (1993) Oxygen free radicals and metallothionein. Free Radical Biol Med 14:325–337

Schultze P, Worgotter E, Braun W, Wagner G, Vasak M, Kagi JH, Wuthrich K (1988) Conformation of $[Cd_7]$-metallothionein-2 from rat liver in aqueous solution determined by nuclear magnetic resonance spectroscopy. J Mol Biol 203:251–268

Shannon RD (1976) Revised effective ionic radii and systematic studies of interatomic distances in halides and chalcogenides. Acta Crystallogr Sect B 32:751–767

Shannon RD, Prewitt CT (1969) Effective ionic radii in oxides and fluorides. Acta Crystallogr Sect B 25:925–946

Simonet V, Calzavara Y, Hazemann JL, Argoud R, Geaymond O, Raoux D (2002) Structure of aqueous $ZnBr_2$ solution probed by X-ray absorption spectroscopy in normal and hydrothermal conditions. J Chem Phys 116: 2997–3006

St Croix CM, Wasserloos KJ, Dineley KE, Reynolds IJ, Levitan ES, Pitt BR (2002) Nitric oxide-induced changes in intracellular zinc homeostasis are mediated by metallothionein/thionein. Am J Physiol Lung Cell Mol Physiol 282:L185–L192

Suzuki KT, Imura N, Kimira M (1993) Metallothionein III. Biological roles and medical implications. Birkhäuser, Basel

Teo BK (1986) EXAFS: basic principles and data analysis. Springer, Berlin Heidelberg New York